

Current Trends in OMICS (CTO)

Volume 5 Issue 1, Spring 2025

ISSN_(P): 2790-8283, ISSN_(E): 2790-8291

Homepage: <https://journals.umt.edu.pk/index.php/cto>



Article QR



Title: Characterization of Nicotine Degradation Associated Proteins in *Paenarthrobacter nicotinovorans*: An In-Silico Analysis

Author (s): Fatima Muccee

Affiliation (s): University of the Punjab, Lahore, Pakistan

DOI: <https://doi.org/10.32350/cto.51.01>

History: Received: December 01, 2024, Revised: January 04, 2025, Accepted: January 29, 2025,
Published: March 05, 2025

Citation: Muccee F. Characterization of nicotine degradation associated proteins in *Paenarthrobacter nicotinovorans*: an in-silico analysis. *Curr Trend OMICS*. 2025;5(1):1–15. <https://doi.org/10.32350/cto.51.01>

Copyright: © The Authors

Licensing:  This article is open access and is distributed under the terms of [Creative Commons Attribution 4.0 International License](#)

Conflict of Interest: Author declared no conflict of interest



A publication of

The Department of Life Sciences, School of Science
University of Management and Technology, Lahore, Pakistan

Characterization of Nicotine Degradation Associated Proteins in *Paenarthrobacter nicotinovorans*: An *In-Silico* Analysis

Fatima Muccee*

School of Biochemistry and Biotechnology, University of the Punjab, Lahore, Pakistan

ABSTRACT

Use of nicotine degrading bacteria (NDB) to degrade nicotine from tobacco waste contaminated soil is emerging as the most promising strategy. In the current study, three nicotine degradation associated proteins from NDB *Paenarthrobacter nicotinovorans* i. e., nicotine dehydrogenase (ndhA), 6-hydroxypseudooxynicotine dehydrogenase (kdhL), and nicotine blue oxidoreductase (nboR) were characterized. For this purpose, coding sequences (CDS) were retrieved from Uniprot database. These sequences were subjected to analysis via PROTPARAM tool, Multiple Em for Motif Elicitation (MEME) suite, SOPMA, SwissModel, Transmembrane Topology Prediction and Classification (TMHMM), and Peptide cutter software. Characterization revealed values of alpha helix, extended strands, and random coil ranging between (29-44%), (14.49-21.08%), and (40.99-53.65%), respectively. Instability index, aliphatic index, and grand average of hydropathy (GRAVY) were observed as 26.76-44%, 91.06-101.32%, and -0.176- 0.091%, respectively. All the proteins exhibited highly complex 3D configuration and multiple number of conserved protein motifs. The number of cleavage sites analyzed for nghA, kdhL, and nboR was 515, 1313, and 313, respectively. The characteristics explored in the current study might be used to modify these proteins in order to maximize nicotine removal from environmental sources.

Keywords: Conserved, motifs, nicotine, *Paenarthrobacter nicotinovorans*, transmembrane domain

1. INTRODUCTION

Nicotine is found in cigarette smoke and is sourced from leaves of tobacco plants, where it is found as an alkaloid [1, 2]. Inhalation of one cigarette smoke causes 1 to 1.5 mg of nicotine to travel in lungs, blood, and brain, resulting in addiction-related effects. Nicotine addiction is a cyclic

*Corresponding Author: fatima.sbb@pu.edu.pk

process which comprises of its absorption, arousal of mood modulation pleasure, physical dependence, withdrawal symptoms on drug abstinence and craving for nicotine, thus self-medicating withdrawal symptoms [3]. Once inside the liver, nicotine undergoes metabolic degradation. About 75% of nicotine is degraded via 5' hydroxylation into 5'-hydroxy nicotine which is then converted into cotinine in the presence of aldehyde oxidase. Cotinine is glucuronidated and released from body as part of urine [4]. Remaining 25% nicotine undergoes 2' hydroxylation and is converted into 2'-hydroxynicotine which is then transformed into 4-methylamino-1, 3-pyridyl-1-butanone (NNK). The NNK is further converted into ketone acids via nitrosation reactions [5].

Once inside the human body, nicotine causes deleterious effects, such as enhancement of cytopathic effects caused by SARS-COV-2 [6], congenital anomalies, and developmental delays [7, 8], cardiovascular, endocrine, immune system and pulmonary disorders, diabetes and cancer [9].

To reduce the human exposure to nicotine and its subsequent hazardous effects, it should be remediated from the environment. Complicated operations and equipments and poor degradation are the limitations of physicochemical remediation strategies. In comparison, bioaugmentation is considered superior due to the involvement of simpler technology, recyclability, and low cost [10]. Several bacteria and fungi have been explored for their biodegradation potential of nicotine for the implementation in bioremediation.

Nicotine degrading bacteria (NDB) reported in literature include *Stenotrophomonas geniculata* ND16 and *Arthrobacter nitrophenolicus* ND6 [11], *Agrobacterium nicotinovorans*, *Pseudomonas putida* S16 and *Agrobacterium tumefaciens* S33 [12], *Bacteroides xylanisolvans* [13], *Bacillus altitudinis* J54 [14], *Bacillus* sp. YC7 [15] and *Pseudomonas fluorescens* strain 1206 [16].

So far, three nicotine degrading pathways have been explored in NDB i. e., pyridine pathway, pyrrolidine pathway, and a variation of the pyridine and pyrrolidine (VPP) pathway. First two pathways mainly occur in *Arthrobacter* and *Pseudomonas*, respectively [10]. Proteins associated with these pathways have been identified which include molybdenum nicotine dehydrogenase (NdhMSL), 6-hydroxy-L-nicotine oxidase (6Hlno),

heterotrimeric ketone hydrogenase (KdhMSL), 2, 6-dihydroxypseudooxynicotine hydrolase (Ponh), 2, 6-dihydroxypyridine-3-hydroxylase (Dphh), 2, 3, 6THP hydrolase (HpoH), 2-ketoglutaramate amidase (HpoI), 4-methylaminobutyrate oxidase (MABO), amine oxidase/monoamine oxidase (AO/MAO), succinic semi-aldehyde dehydrogenase (SsaDH), nicotine oxidoreductase (NicA2), pseudooxynicotine amidase (Pnao), 3-succinoylsemialdehyde pyridine dehydrogenase (Sapd), 3-succinoylpyridine monooxygenase (SpmABC, 6-hydroxy-3-succinoyl pyridine hydroxylase (HspB), N-formylmaleamate deformylase (Nfo), maleamate amidohydrolase (Ami), maleate cis/trans isomerase (Iso), and 6-HPON amine oxidase (HisD) [17]. Additionally, five key proteins. i. e., nicotine dehydrogenase (ndhA), (S)-6-hydroxynicotine oxidase (nctB), 6-hydroxypseudooxynicotine dehydrogenase (kdhL), nicotine blue oxidoreductase (nboR), and 2,6-dihydroxypseudooxynicotine hydrolase (dhponh), were reported while investigating the rhizospheric dwelling NDB *Paenarthrobacter nicotinovorans* [11].

The current study was conducted keeping in view the health hazards associated with nicotine and limited knowledge about the proteins associated with its degradation. Three nicotine degradation associated bacterial proteins were selected i.e., ndhA, kdhL, and nboR for detailed characterization. Analyzing the properties of these proteins might help in manipulating them to enhance their expression and role in nicotine breakdown.

2. METHOD

2.1. Proteins Sequence Retrieval-Uniprot Database

To retrieve the sequences of proteins i.e., ndhA, kdhL, and nboR, Uniprot database (<https://www.uniprot.org/>, accessed on 31st July 2024) was accessed. The accession IDs of proteins and their sequences are shown in Supplementary Data Table S1.

2.2. Physicochemical Properties

PROTPARAM tool (<https://web.expasy.org/protparam/>, accessed on 31st July 2024) was consulted to analyze the physicochemical properties of proteins documented in present study. The properties documented included number of amino acids, molecular weight, isoelectric point (pI), extinction coefficient, instability index, aliphatic index, and GRAVY.

2.3. Primary Structure Analysis

Multiple Em for Motif Elicitation (MEME) suite 5.5.5 (<https://meme-suite.org/meme/tools/meme>, accessed on 31st July 2024) was used to predict the conserved protein motifs of nicotine degradation associated proteins.

2.4. Secondary Structure Analysis

SOPMA protein secondary structure prediction, Network Protein Sequence Analysis (NPS@) server (https://npsa.lyon.inserm.fr/cgi-bin/npsa_automat.pl?page=/NPSA/npsa_sopma.html, accessed on 31st July 2024) was employed to predict the secondary (2D) configuration of proteins.

2.5. Tertiary Structure Analysis

ExPasy homology modelling web server, SWISSMODEL (<https://swissmodel.expasy.org/interactive>, accessed on 1st August 2024) was consulted to predict the tertiary (3D) configuration of current study proteins.

2.6. Functional Analysis

Deep Learning model for Transmembrane Topology Prediction and Classification (TMHMM) 1.0.39 tool (www.cbs.dtu.dk/services/TMHMM, accessed on 1st August 2024) was employed to predict membrane topology and level of configuration of the current study proteins. To identify the disordered sequences in proteins, GlobPlot 2.3 (<http://globplot.embl.de/>, accessed on 1st August 2024) was consulted. Peptide characterization software, Peptide cutter (http://web.expasy.org/peptide_cutter/, accessed on 1st August 2024) was used for proteolytic cleavage sites prediction.

3. RESULTS

3.1. Prediction of Physicochemical Properties

The kdhL protein was the longest with 794 amino acids. Highest pI (6.58) was observed in nboR (Table 1). Half-life was same in all three proteins. The extinction coefficient was highest (68425) in kdhL protein. The highest (44) and lowest (26.76) values of instability index were found in ndhA and nboR, respectively. Aliphatic index was comparable among the three documented proteins. The kdhL exhibited very small value for GRAVY as compared to ndhA (0.011) and nboR (0.091).

Table 1. Prediction of Physicochemical Properties of Current Study Proteins using PROTPARAM Tool

Protein	No. of amino acid	Molecular wt.	pI	Extinction coefficients	Half life	Instability index	Aliphatic index	GRAVY
ndhA	283	30011.12	5.40	26930	>10 hr	44	98.98	0.011
kdhL	794	86370.70	5.14	68425	>10 hr	34.35	91.06	-0.176
nboR	204	21536.67	6.58	18700	>10 hr	26.76	101.32	0.091

3.2. Prediction of Primary Structure

In protein ndhA, ten conserved motifs. i. e., HPQIRN, HATIVN, KHLPM, FVGPYPM, NGWGYGEF, HGDAAGEW, NGMVEVQ, MAMRLAQ, DACDLLSTDEDSK, and DAEDVLNGSELSP with p-values of 3.41e-9, 2.49e-7, 1.10e-8, 2.93e-8, 2.06e-11, 5.10e-9, 1.26e-9, 1.20e-7, 3.47e-16, and 1.19e-12, respectively were found. In protein kdhL, eleven motifs. i. e., MPNVDCF, MNNAMNY, QLHMRIV, QIFSRCQ, QAHARIV, MKDEIFHNHGAYFRQ, GYHEIYENIEDFSHP, GSFKVK, GSFGVK, NFSEWL, and SFMDYL with p-values 9.31e-11, 1.46e-9, 3.66e-9, 8.45e-9, 2.50e-8, 4.27e-18, 2.05e-16, 1.38e-8, 4.92e-8, 6.32e-9, and 1.40e-7, respectively were predicted. In protein nboR, ten motifs. i. e., FLRQKPWLVDLIDCSDESTGE, CARANLEPYRIVVNHDWSSGM, HTKNHI, HRPGRI, DTVEQM, DAAETM, CHEVVI, GHPMVI, MGDTDLPC, and YSSLDSPR with p-values 1.07e-23, 3.30e-21, 3.28e-9, 9.41e-8, 6.26e-9, 2.17e-7, 1.85e-8, 5.63e-8, 1.46e-10, and 1.90e-7, respectively were found. (Figure 1 and Table 2).

Table 2. Conserved Motif Sequences of the current Study Proteins, their E-values, and P-values Predicted based on MEME Suite

No. of domains	E-value	p-value	Conserved Domain Sequences
ndhA			
1	3.8e+001	3.41e-9	MMAAAGRHIA HPQIRN RGTLGGSLAH
2		2.49e-7	DYVRFGPMVT HATIVN SPAVAKHPLM
3	1.8e+001	1.10e-8	ATIVNSPAVA KHLPM AAAGRHIAHP

No. of domains	E-value	p-value	Conserved Domain Sequences			
4		2.93 e-8	GRRTIEADDL	FVGPYM	TSLAADEIIT	
5	9.1e+	2.06 e-11	ITDVWIPSRP	NGWGYGEF	ARRSGDYGLA	
6	001	5.10 e-9	NRGTLGGSLA	HGDAAGEW	PLVLLALNGM	
7	3.3e+	1.26 e-9	GEWPLVLLAL	NGMVEVQ	SVRGRRTIEA	
8	002	1.20 e-7	IAGGQSLLPV	MAMRLAQ	PSVVIDLGNV	
9	3.7e+	3.47 e-16	IRYASPASIE	DACDLLSTDEDISK	IIAGGQSLLP	
10	002	1.19 e-12	GAVGKIQRVP	DAEDVLNGSELSP	ERAEAASEAG	
kdhL						
1	1.1e+	9.31 e-11	MDYLLPSAQE	MPNVDCF	VTEDAKSPDN	
2	000	1.46 e-9	EPGLAADAVY	MNNAMNY	PYGVTLVQIE	
3		3.66 e-9	TFAGDLGVPG	QLHMRIV	RSTQAHARIV	
4	2.6e+	8.45 e-9	HTDRLPVTPE	QIFSRCQ	GLNKAER	
5	001	2.50 e-8	QLHMRIVRST	QAHARIV	SIDATEAEKT	
6	2.8e+	4.27 e-18	ALDAEGRILG	MKDEFHNHGAYFRQ	AEPLVSDITA	
7	002	2.05 e-16	HLGSVLLEEL	GYHEIYENIEDFSHP	VLAVDKVLVY	
8	3.3e+	1.38 e-8	ADPDDELTA	GSFKVK	GTDQQISLYE	
9	002	4.92 e-8	NVRMKHVEIG	GSFGVK	GGVFPEENVVA	
10	2.5e+	6.32 e-9	KHFNEALEAA	NFSEWL	EESKRLRADG	
11	002	1.40 e-7	YEEDGQPITT	SFMDYL	LPSAQEMPNV	
nboR						
1	7.3e+	1.07 e-23	TVSGDAGA	FLRQKPWLVDLIDCSDES	DVDTVEQM	
	000	RV		TGE	YR	
2		3.30 e-21	IVLGANAQ	CARANLEPYRIVVNHDWS	GSSYLAGD	
		AV		SGM	AA	
3	4.2e+	3.28 e-9	SSYLAGDAAA	HTKNHI	LVALVDQPG	
	001	9.41 e-8	VTTVGRLLV	HRPGRI	SSAAYSSLDS	

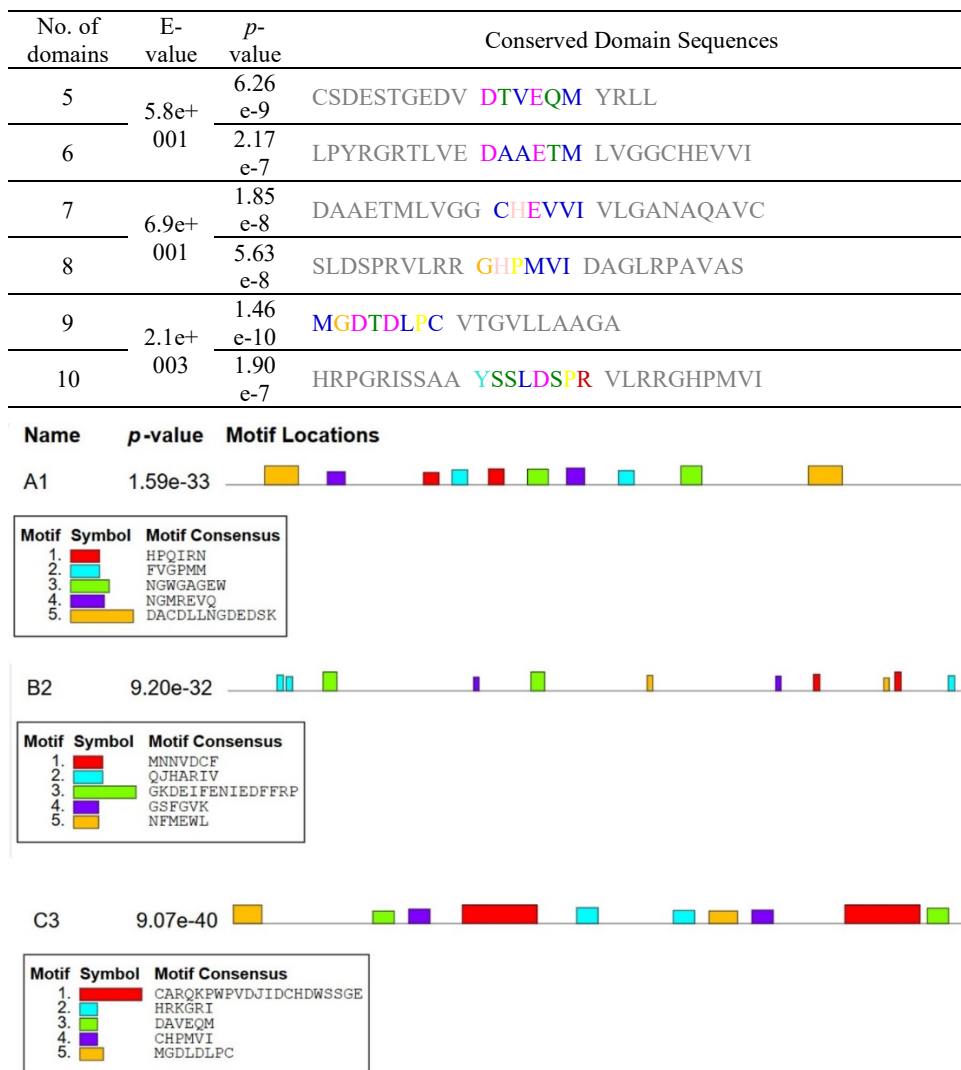


Figure 1. Assessment of Conserved Motifs of the Current Study Proteins using MEME Suite

3.3. Prediction of Secondary (2D) Structure

Three aspects of 2D structure were addressed i. e., alpha helix, extended strand, and random coil. Highest values for all these aspects were observed in kdhL as compared to other two (Table 3, Figure 2). Lowest number of amino acids (70) participating in alpha helix formation were found in nboR.

Least number of amino acids (16) forming random coil were observed in ndhA.

Table 3. Prediction of 2D Configuration of Proteins Documented in the Current Study using SOPMA Tool

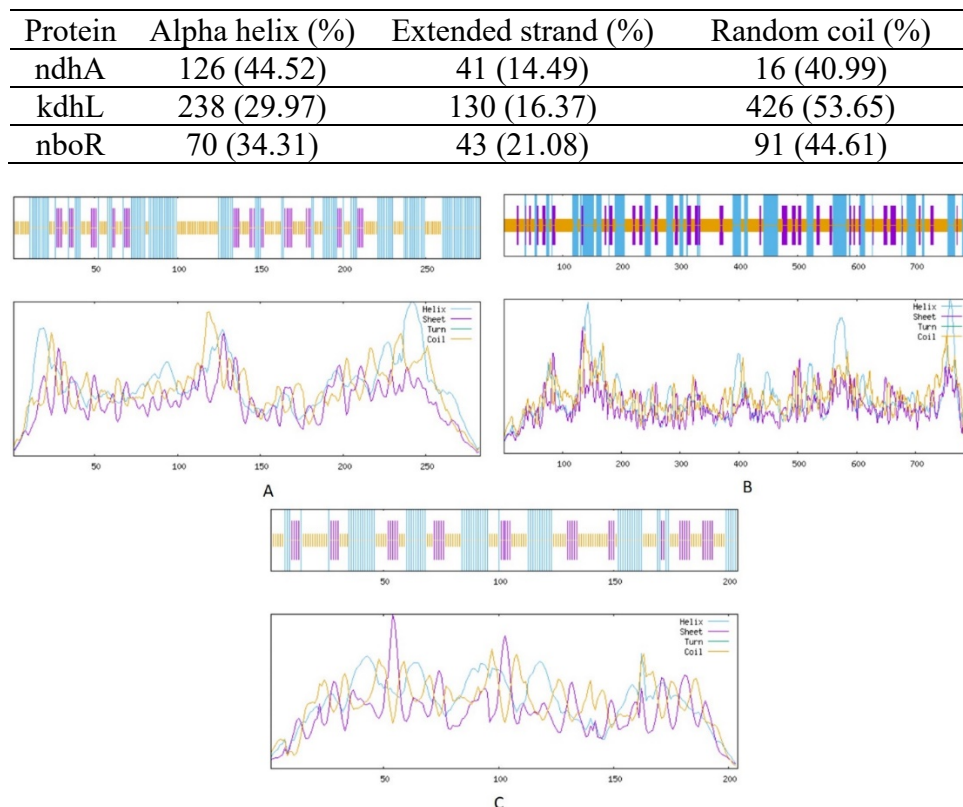


Figure 2. Secondary Structure Assessment of the Current Study Proteins via SOPMA Tool

(A) ndhA (B) kdhL (C) nboR

3.4. Prediction of Tertiary (3D) Structure

The 3D configuration revealed complex tertiary configuration in all three proteins. However, the kdhL exhibited highest complex level of folding followed by ndhA and then nboR (Figure 3).

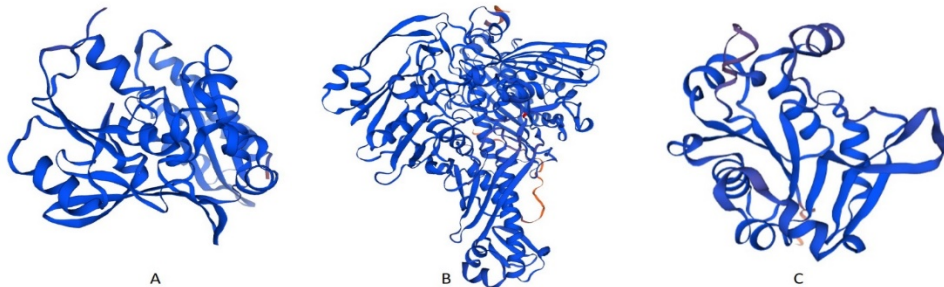


Figure 3. Prediction of 3D Configuration of Proteins Documented in the Current Study using SWISSMODEL. (A) ndhA (B) kdhL (C) nboR

3.5. Prediction of Functional Aspects

The transmembrane domain analysis revealed that all three proteins were localized inside the cell without any transmembrane domain (Supplementary Data Figure S1).

Non-disordered sequence was observed in ndhA protein ranged from 108-118 (RGTLGGSLAHG), 171-185 (IPSRPNGWGYGEFAR), and 279-283 (AGART). In kdhL, this region was found in amino acids 9-19 (IPDNGRAGADE), 45-49 (FAGDL), 268-274 (SFGVKGG), 427-435 (PGLDIVHEP), 505-510 (KTGGSS), 543-554 (LIPDGVGWSRR), 619-624 (ARADND), and 730-745 (V TEDAKSPDNP FGAKG). In nboR, non-ordered amino acids found were 1-10 (MGDTDLPCVT), 22-28 (LGRGPKA), and 81-90 (WSSGMGSSYL) (Figure 4).

In ndhA protein, multiple number of cleavage sites were observed i. e., 21 sites (Arg-C proteinase), 17 (Asp-N endopeptidase, 34 (Asp-N endopeptidase⁺ N terminal Glu), 34 (Asp-N endopeptidase⁺ N terminal Glu), 3 (BNPS-Skatole), 8 (CNBR), 1 (Caspase 10), 12 (Chymotrypsin-low specificity), 48 (Chymotrypsin-high specificity), 21 (Clostripain), 17 (Glutamyl endopeptidase), 37 (pepsin), 2 (proline endopeptidase), 146 (proteinase K), 89 (Thermolysin), and 25 (Trypsin). In protein kdhL, 52 cleavage sites were observed. i. e. (Arg-C proteinase), 49 (Asp-N endopeptidase), 2 (Caspase-1), 50 (Chymotrypsin-high specificity), 145 (Chymotrypsin-low specificity), 67 (Glutamyl endopeptidase), 121 (Pepsin), 1 (Proline endopeptidase), 434 (Proteinase K), 61 (Staphylococcal peptidase I), 251 (Thermolysin), 1 (Thrombin), and 79 (Trypsin). In nboR, 16 sites were observed i. e. (Arg-C proteinase), 14 (Asp-N endopeptidase), 8 (Chymotrypsin-high specificity), 38 (Chymotrypsin-low specificity), 7

(Glutamyl endopeptidase), 28 (Pepsin), 4 (Proline-endopeptidase), 101 (Proteinase K), 7 (Staphylococcal peptidase I), 72 (Thermolysin), 1 (Thrombin), and 17 (Trypsin).

```
>none_Disorder 108-118, 171-185, 279-283
mklpairyrs pasiedacd1 lstdedskii aggqsllpvm amrlaqpsvv idlgnvpglt rleevgdyvr fgpmvthati vnspacevahl pmmaaagrhi ahpqirnRGT
LGGSLAHdga agepwlvlla lmgmvevqsv rgrtiveadd lfvgpymts1 aadeiitdw IPSRPNGWGY GEFAReRsgdy gianvavvis tadsrisdvr iavggavki
qrvpdaedvl ngselspera eaaseagaks lsyisdihg5 aeyrghlvqe lirrtiveAG ART
```

A

```
>none_Disorder 9-19, 45-49, 268-274, 427-435, 505-510, 543-554, 619-624, 730-745
mmakalip DNGRAGADEG nrqawigev lrredrllt gtatFAGDLG vpglmhrii rsgqahariv sidateakt pgvrmvitse htrhlgsvll eelgheheiye
niedfshpvl avdkvlyvgq pvvavladp lyeadaelv sieyeplplv ldpealgtk velfgrgne garikkaygd idrafaeaeah virhkyvtnt hsgvpmepra
vvvpqdpard tlfliwgtvh hnrrriiakm lnipevnrm kheviggSFG VKGGvfpenv vaawartg vpkwtedrv ehmtstshar emvhkileal daegrlgmk
deifnnhngay frqaepivsd itaglifgpy rvpaydatlh avftnktpvg aypagrynes tfarerifol acaeiglsvt efrrrnlita edlptwPGLD IVHEPyhfd5
gdvkhfneea leaanfswl eeskradg rkvgvlgv1 mdakaglgfpe tggvevrag rvtVKTGSSS vgagietvla qivaeelqia penidivhsd telIPDGVS
WSSRstvlag gaarkaalav vekarrlase mleapddle itagsfkvgk tddqislyei aaardpftar AODDepglaa davymnnamn ypygvtlvqi eldpdtgghr
ilrfststea grvinpltr gqiigavqg iggalyeefl yeedgapitt sfmdyllpsa qemppnvdctv TEDAKSPDNP FGAKGlgcig iiaagaaiaas aiddaiadgv
htdrlpvpte qifsrcqgln kaer
```

B

```
>none_Disorder 1-10, 22-28, 81-90
MGDTDLPCVT gvllaaagakg rLGRGPKAII pyrgrtlved aetmlvggc hevvivlgan aqavcaranl epyrivrnhd WSSGMGSSYL agdaaaahtkn hilvalvdqp
glsvttvgrl lvshprgris saayssldsp rvlrrghpmv idaglrpava stvsgdagar vflrqkpw1 dlidcsdest gedvdvtveqm yr11
```

C

Figure 4. Prediction of Non-disordered Amino Acid Sequences in the Current Study Proteins via GlobPlot. (A) ndhA (B) kdhL (C) nboR

4. DISCUSSION

In the current study, nicotine degradation associated proteins of *Paenarthrobacter nicotinovorans* were targeted. It is gram positive NDB. Several strains of this bacterium have been characterized and explored for nicotine metabolism in literature [18–22]. With the help of nicotine inducible gene (nic) cluster, it may use nicotine as carbon and energy source. The nic cluster encodes enzymes nicotine dehydrogenase (ndh), 6-hydroxy-L-nicotine oxidase (6HLNO), 6-hydroxy-D-nicotine oxidase (6HDNO), ketone dehydrogenase (kdh), 2, 6-dihydroxypseudooxynicotine hydrolase (DHPONH), 2,6-dihydroxypyridine-3-hydroxylase (DHPH), nicotine blue oxidoreductase (nboR), Y-N-methylaminobutyrate oxidase (MABO), methylene tetrahydrofolate dehydrogenase (Fold), formyltetrahydrofolate deformylase (PurU), monoamine oxidase (MAO), succinic semialdehyde dehydrogenase (SsaDH), putative polyketide cyclase (PKC), and omega amidase (NIT) [21].

Pathway of nicotine degradation in *P. nicotinovorans* was explored [21]. According to this pathway, initially, L-nicotine is hydroxylated into 6-hydroxynicotine (6-HNic) in the presence of nicotine dehydrogenase (NDH). This step is followed by the formation of 6-hydroxyl methylmyosamine (6-HMM). Reaction is catalyzed by 6-hydroxy-D-

nicotine oxidase (6-HDNO) and 6-hydorxy-L-nicotine oxidase (6-HLNO). Afterwards, 6-HMM is hydrated and 6-hydroxyl-pseudooxynicotine (6-HPON) is formed. The 6-HPON is hydroxylated into 2,6-dihydroxypeudooxynicotine (2,6-DHPON) in the presence of ketone dehydrogenase (KDH). 2,6-dihydroxypseudooxynicotine hydrolase (DHPONH) catalyzes the transformation of 2,6-dihydroxypeudooxynicotine (2,6-DHPON) into 2,6-dihydroxypyridine (2,6-DHP). This is followed by the formation of 2,3,6-trihydroxypyridine (2,3,6-THP) in the presence of 2,6-dihydroxypyridine-3-hydroxylase (DHPH) through hydroxylation. The 2,3,6-THP is oxidized into leuco form of nicotine blue which may be further processed either spontaneously or in the presence of nicotine blue oxidoreductase (NBOR). Then, putative polyketide cyclase (PKC) catalyzed the transformation of nicotine blue into alpha keto-glutaramate (alpha-KGA) which is converted into alpha-ketoglutarate (alpha-KG). The alpha-KG ultimately enters into krebs cycle.

Among these nic cluster proteins, *ndhA*, *kdhL*, and *nboR* were documented in the current study. In the current investigation, the molecular wt. of *ndhA* was found 30011.12 which is consistent with previous study reporting the same value for this subunit of *ndh* protein [23]. Isoelectric point (pI) reflects the alkaline or acidic nature of protein. The *ndhA* and *kdhL* were acidic with pI of 5.40 and 5.14, while *nboR* was found slightly alkaline with pI close to 7 [24]. Instability index value below 40 reflects the stable nature of protein [25]. According to this study, *kdhL* and *nboR* were stable as compared to *ndhA* protein. Aliphatic index value was directly related with the thermostability of protein and the values documented in the current study indicated high thermostability of all the three documented proteins [26]. All these proteins were thermostable with aliphatic index ranging between 91.06 and 101.32.

4.1. Conclusion

The exploration of nicotine degradation pathways associated proteins might help in the manipulation of these proteins. Moreover, the enzymes may be purified to produce nanoparticles or the desired genes can be cloned into eco-friendly expression systems. Extracellular and intracellular enzymes associated with nicotine degradation can be purified and coated on nanoparticles. These nanoparticles enhance the efficiency of enzymes via immobilization. Hence, the enzymes might contribute to sustainable green remediation of nicotine.

CONFLICT OF INTEREST

The authors of the manuscript have no financial or non-financial conflict of interest in the subject matter or materials discussed in this manuscript.

DATA AVAILABILITY STATEMENT

The CDS of proteins documented in the current study are available at Uniprot database.

FUNDING DETAILS

No fundings were received for this research.

REFERENCES

1. Pandey SK, Vishwakarma PK, Yadav SK, Shukla P, Srivastava A. Multiwalled carbon nanotube filters for toxin removal from cigarette smoke. *ACS Appl Nano Mater.* 2019;3(1):760–771. <https://doi.org/10.1021/acsanm.9b02277>
2. Wei H, Rui J, You M, et al. Materials for the selective removal of toxic compounds in cigarette smoke: a review. *Sep Purif Technol.* 2024:e128908. <https://doi.org/10.1016/j.seppur.2024.12890>
3. Ma C, Liu Y, Neumann S, Gao X. Nicotine from cigarette smoking and diet and Parkinson disease: a review. *Transl Neurodegener.* 2017;6:1–7. <https://doi.org/10.1186/s40035-017-0090-8>
4. Hecht SS, Hochalter JB, Villalta PW, Murphy SE. 2'-Hydroxylation of nicotine by cytochrome P450 2A6 and human liver microsomes: formation of a lung carcinogen precursor. *Proc Natl Acad Sci USA.* 2000;97(23):12493–12497. <https://doi.org/10.1073/pnas.220207697>
5. Hirata N, Yamada S, Sekino Y, Kanda Y. Tobacco nitrosamine NNK increases ALDH-positive cells via ROS-Wnt signaling pathway in A549 human lung cancer cells. *J Toxicol Sci.* 2017;42(2):193–204. <https://doi.org/10.2131/jts.42.193>
6. Sansone L, Milani F, Fabrizi R, et al. Nicotine: from discovery to biological effects. *Int J Mol Sci.* 2023;24(19):e14570. <https://doi.org/10.3390/ijms241914570>
7. Blanc J, Tosello B, Ekblad MO, Berlin I, Netter A. Nicotine replacement therapy during pregnancy and child health outcomes: a systematic review. *Int J Environ Res Public Health.* 2021;18(8):e4004. <https://doi.org/10.3390/ijerph18084004>

8. McGrath-Morrow SA, Gorzkowski J, Groner JA, Rule AM, Wilson K, Tanski SE, et al. The effects of nicotine on development. *Pediatrics*. 2020;145(3):e20191346. <https://doi.org/10.1542/peds.2019-1346>
9. Gould TJ. Epigenetic and long-term effects of nicotine on biology, behavior, and health. *Pharmacol Res*. 2023;192:e106741. <https://doi.org/10.1016/j.phrs.2023.106741>
10. Zhang Z, Mei X, He Z, et al. Nicotine metabolism pathway in bacteria: mechanism, modification, and application. *Appl Microbiol Biotechnol*. 2022;106(3):889–904. <https://doi.org/10.1007/s00253-022-11763-y>
11. Wang Y, Luo X, Chu P, et al. Cultivation and application of nicotine-degrading bacteria and environmental functioning in tobacco planting soil. *Bioresour Bioprocess*. 2023;10(1):e10. <https://doi.org/10.1186/s40643-023-00630-x>
12. Liu J, Ma G, Chen T, et al. Nicotine-degrading microorganisms and their potential applications. *Appl Microbiol Biotechnol*. 2015;99:3775–3785. <https://doi.org/10.1007/s00253-015-6525-1>
13. Chen B, Sun L, Zeng G, et al. Gut bacteria alleviate smoking-related NASH by degrading gut nicotine. *Nature*. 2022;610(7932):562–568. <https://doi.org/10.1038/s41586-022-05299-4>
14. Jiang Y, Gong J, Chen Y, et al. Biodegradation of nicotine and TSNA by *Bacterium* sp. strain J54. *Iran J Biotechnol*. 2021;19(3):e2812. <https://doi.org/10.30498/ijb.2021.240460.2812>
15. Zhang K, Yin M, Lei S, Zhang H, Yin X, Niu Q. *Bacillus* sp. YC7 from intestines of *Lasioderma serricorne* degrades nicotine due to nicotine dehydrogenase. *AMB Express*. 2023;13(1):e87. <https://doi.org/10.1186/s13568-023-01593-0>
16. Xia Z-Y, Yu Q, Lei L-P, et al. A novel nicotine-degrading bacterium *Pseudomonas fluorescens* strain 1206. *Appl Biochem Microbiol*. 2019;55(2):123–128.
17. Mu Y, Chen Q, Parales RE, et al. Bacterial catabolism of nicotine: catabolic strains, pathways and modules. *Environ Res*. 2020;183:e109258. <https://doi.org/10.1016/j.envres.2020.109258>
18. El-Sabeh A, Mlesnita A-M, Munteanu I-T, et al. Characterisation of the *Paenarthrobacter nicotinovorans* ATCC 49919 genome and identification of several strains harbouring a highly syntenic *nic*-genes cluster. *BMC Genomics*. 2023;24(1):e536.
19. Mihăsan M, Boiangiu RzSt, Guzun D, et al. Time-dependent analysis of *Paenarthrobacter nicotinovorans* pAO1 nicotine-related proteome.

ACS *Omega*. 2021;6(22):14242–14251.
<https://doi.org/10.1021/acsomega.1c01020>

20. Mihăsan M, Babii C, Aslebagh R, Channaveerappa D, Dupree EJ, Darie CC. Exploration of nicotine metabolism in *Paenarthrobacter nicotinovorans* pAO1 by microbial proteomics. *Adv Mass Spectrom Biomed Res*. 2019:515–529. https://doi.org/10.1007/978-3-030-15950-4_30

21. Mihăsan M, Babii C, Aslebagh R, Channaveerappa D, Dupree E, Darie CC. Proteomics-based analysis of the nicotine catabolism in *Paenarthrobacter nicotinovorans* pAO1. *Sci Rep*. 2018;8(1):e16239. <https://doi.org/10.1038/s41598-018-34687-y>

22. Mujawar SY, Shamim K, Vaigankar DC, Naik MM, Dubey SK. Rapid arsenite oxidation by *Paenarthrobacter nicotinovorans* strain SSBW5: unravelling the role of *GlpF*, *aioAB*, and *aioE* genes. *Arch Microbiol*. 2023;205(10):e333. <https://doi.org/10.1007/s00203-023-03673-y>

23. Grether-Beck S, Igloi GL, Pust S, Schilz E, Decker K, Brandsch R. Structural analysis and molybdenum-dependent expression of the pAO1-encoded nicotine dehydrogenase genes of *Arthrobacter nicotinovorans*. *Mol Microbiol*. 1994;13(5):929–936. <https://doi.org/10.1111/j.1365-2958.1994.tb00484.x>

24. Audain E, Ramos Y, Hermjakob H, Flower DR, Perez-Riverol Y. Accurate estimation of isoelectric point of protein and peptide based on amino acid sequences. *Bioinformatics*. 2016;32(6):821–827. <https://doi.org/10.1093/bioinformatics/btv674>

25. Gamage DG, Gunaratne A, Periyannan GR, Russell TG. Applicability of instability index for in vitro protein stability prediction. *Protein Pept Lett*. 2019;26(5):339–347. <https://doi.org/10.2174/0929866526666190228144219>

26. Morya VK, Yadav S, Kim E-K, Yadav D. *In silico* characterization of alkaline proteases from different species of *Aspergillus*. *Appl Biochem Biotechnol*. 2012;166:243–257. <https://doi.org/10.1007/s12010-011-9420-y>